

# Bounds on the longitudinal and shear wave attenuation ratio of polycrystalline materials (L)

Christopher M. Kube<sup>a)</sup>

Weapons & Materials Research Directorate, U.S. Army Research Laboratory, Building 4600, Aberdeen Proving Ground, Maryland 21005-5069, USA

#### Andrew N. Norris

Mechanical and Aerospace Engineering, Rutgers University, Piscataway, New Jersey 08854, USA

(Received 1 February 2017; revised 22 March 2017; accepted 28 March 2017; published online 13 April 2017)

A lower bound to the longitudinal and shear attenuation ratio was recently derived for viscoelastic materials [Norris, J. Acoust. Soc. Am. **141**, 475–479 (2017)]. This letter provides proof that a similar bound is present for low-frequency attenuation constants of polycrystals caused by grain scattering. An additional upper bound to the attenuation ratio is unveiled. Both bounds are proven to be combinations of wave speeds. The upper and lower bounds correspond with the vanishing of the second-order anisotropy of the bulk and shear modulus, respectively. A link to the polycrystalline Poisson's ratio is highlighted, which completely bounds the attenuation ratio. An analysis of 2176 crystalline materials was conducted to further verify the bounds.

© 2017 Acoustical Society of America. [http://dx.doi.org/10.1121/1.4979980]

[JFL] Pages: 2633–2636

#### I. INTRODUCTION

In a recent article, the passivity condition on the absorptive properties of viscoelastic materials was applied to elastic wave propagation. The condition requires that the total energy associated with the wave motion decreases by virtue of the passive absorbing properties of viscoelastic materials. This condition led to the derivation of the inequality.

$$\frac{\alpha_L}{\alpha_S} \ge \frac{4c_S^3}{3c_L^3},\tag{1}$$

which is valid when the imaginary or dissipative part of the wavenumber is much smaller than its real part. The right-hand side of Eq. (1) is the ratio of longitudinal and shear wave speeds denoted as  $c_L$  and  $c_S$ , respectively. In general, the shear modulus and bulk modulus both contribute to the absorption. It is those cases in which the absorption is attributable to the shear modulus only that Eq. (1) yields the lower limit.

The derivation of Eq. (1), based on viscoelastic materials, led naturally to the question of whether this inequality holds more generally. In other words, does Eq. (1) hold for attenuations that result from other physical mechanisms like scattering or other material systems that are not viscoelastic. In this letter, we partially answer this question by considering the scattering based attenuation of polycrystalline materials.

## II. THEORY

In polycrystalline materials, the crystallites are often referred to as grains that consist of the constituent material. These grains have various morphologies and crystallographic orientations depending on their crystallization histories. It is dissimilar orientations and orientation-dependent single-crystal elastic behavior that causes the interface or grain boundary between adjacent grains to scatter wave energy. For an incident wave in a polycrystal, the scattering based attenuation is the net energy that is removed (scattered) out of the primary wave by all scattering events. The resulting wave energy after the scattering occurs is a combination of the remaining incident wave, which has decreased in amplitude, and a scattered secondary field. The total attenuation of waves in polycrystals consists of contributions of scattering and absorption. However, the effect of absorption, due to physical mechanisms such as dislocation damping and internal friction, are around 2 orders of magnitude less than that of scattering.<sup>2</sup> Thus, the study of attenuation in polycrystals has heavily focused on scattering and will be the focus of this letter.

Attenuation and scattering of waves in polycrystals, both theoretical and experimental, has a rich history.  $^{3-11}$  The topic continues to garner interest because of applications including microstructure characterization, flaw detection, and seismology.  $^{12-17}$  The present theory begins from an extension of Weaver's model  $^{11}$  to isotropic polycrystals consisting of crystallites having general or triclinic crystallographic symmetry.  $^{12}$  The treatment is universal because all crystalline materials contain point group symmetries that are a subset of the triclinic point group. For a wave of angular frequency  $\omega$ , the longitudinal and shear wave attenuations may be written as  $^{11}$ 

$$\alpha_{L} = \frac{\pi^{2} \omega^{4}}{2\rho^{2} c_{L}^{3}} \int_{-1}^{+1} \left[ \frac{\eta^{LL}(\theta)}{c_{L}^{5}} L(\theta) + \frac{\eta^{LS}(\theta)}{c_{S}^{5}} (M(\theta) - L(\theta)) \right] d\cos\theta$$
(2)

a)Electronic mail: christopher.m.kube.ctr@mail.mil

$$\alpha_{S} = \frac{\pi^{2} \omega^{4}}{4 \rho^{2} c_{S}^{3}} \int_{-1}^{+1} \left[ \frac{\eta^{SS}(\theta)}{c_{S}^{5}} (N(\theta) - 2M(\theta) + L(\theta)) + \frac{\eta^{LS}(\theta)}{c_{L}^{5}} (M(\theta) - L(\theta)) \right] d\cos\theta,$$
(3)

respectively. The factors  $\eta^{LL}$ ,  $\eta^{LS}$ , and  $\eta^{SS}$  are spatial Fourier transforms of the microstructure's two-point correlation function, which are found in Eq. (7.3) of Ref. 11. The factors  $L(\theta)$ ,  $M(\theta)$ , and  $N(\theta)$  are inner products on the eighth-rank covariance tensor, which is a measure of the mean squared elastic moduli fluctuations resulting from random grain orientations. These inner products were previously defined for isotropic polycrystals having triclinic crystallites and will be used in the following. The attenuations in Eqs. (2) and (3) assume that the polycrystal is composed of single phase equiaxed crystallites (on average), which do not display preferred orientations. These considerations imply statistical isotropy and homogeneity. Attenuation formulas based on these assumptions have been shown to agree well with experimental measurements.

In many practical cases, the ultrasonic wavelength is sufficiently large such that the attenuation is a result of Rayleigh scattering. Rayleigh attenuations are found from Eqs. (2) and (3) by evaluating the integrals while making the low-frequency (Rayleigh) assumption  $\omega \ell/c_L \ll 1$ , where  $\ell$  is the correlation length of the microstructure. The correlation length at low frequencies is near the average grain radius. <sup>10,11</sup> As an example,  $\omega \ell/c_L \approx 0.05$  for a 5 MHz wave

in steel with a mean grain diameter of  $20 \, \mu m$ . The Rayleigh attenuations are then found to be

$$\alpha_L^{\text{Rayleigh}} = \frac{1}{15} \frac{\ell^3 \omega^4}{\rho^2 c_L^8} \left[ \frac{1}{36} (\beta + 672\mu) + \frac{R^5}{48} (\beta + 1344\mu) \right]$$
(4)

and

$$\alpha_S^{\text{Rayleigh}} = \frac{1}{30} \frac{\ell^3 \omega^4}{\rho^2 c_S^8} \left[ \frac{R^{-5}}{48} (\beta + 1344\mu) + 42\mu \right], \tag{5}$$

where the factors of  $L(\theta)$ ,  $M(\theta)$ , and  $N(\theta)$  were taken from Ref. 12. The factor R is the ratio of the velocities,  $R = c_I/c_S$ .  $\mu = \langle \delta c_{55} \delta c_{55} \rangle$  and  $\beta = 120 \langle \delta c_{13} \delta c_{13} \rangle - 80 \langle \delta c_{15} \delta c_{35} \rangle + 480$  $\langle \delta c_{13} \delta c_{33} \rangle + 135 \langle \delta c_{33} \delta c_{33} \rangle$  are second-order anisotropy constants related to elastic anisotropy of the bulk and shear moduli, respectively. We employ the Voigt index convention in  $\mu$  and  $\beta$ , which contracts pairs of indices in the manner  $\delta c_{iikl} \rightarrow \delta c_{IJ}$  with  $11 \rightarrow 1, 22 \rightarrow 2, 33 \rightarrow 3, 23$  or  $32 \rightarrow 4, 13$ or 31  $\rightarrow$  5, and 12 or 21  $\rightarrow$  6. The first-order elastic moduli variations (in full index notation) are  $\delta c_{ijkl} = c_{ijkl} - \langle c_{ijkl} \rangle$ with  $c_{iikl}$  being the single-crystal elastic modulus tensor and () being an unweighted average over all possible crystallite orientations (often referred to as a Voigt-type average). The second-order elastic moduli variations are defined as  $\langle \delta c_{ijkl} \delta c_{\alpha\beta\gamma\delta} \rangle = \langle (c_{ijkl} - \langle c_{ijkl} \rangle) (c_{\alpha\beta\gamma\delta} - \langle c_{\alpha\beta\gamma\delta} \rangle) \rangle$ . Their evaluation follows from Eq. (3) of Ref. 12. Evaluating the elastic moduli variations give

$$\mu = \frac{1}{1575} \left( 8c_{11}^2 - 16c_{11}c_{12} - 16c_{11}c_{13} + c_{11}c_{22} + 14c_{11}c_{23} + c_{11}c_{33} - 12c_{11}c_{44} - 12c_{11}c_{55} - 12c_{11}c_{66} + 23c_{12}^2 - 14c_{12}c_{13} \right. \\ \left. - 16c_{12}c_{22} - 14c_{12}c_{23} + 14c_{12}c_{33} + 12c_{12}c_{44} + 12c_{12}c_{55} + 12c_{12}c_{66} + 23c_{13}^2 + 14c_{13}c_{22} - 14c_{13}c_{23} - 16c_{13}c_{33} \right. \\ \left. + 12c_{13}c_{55} + 12c_{13}c_{56} + 60c_{14}^2 - 60c_{14}c_{24} - 60c_{14}c_{34} + 60c_{15}^2 - 60c_{15}c_{25} - 60c_{15}c_{35} + 60c_{16}^2 - 60c_{16}c_{26} \right. \\ \left. - 60c_{16}c_{36} + 8c_{22}^2 - 16c_{22}c_{23} + c_{22}c_{33} - 12c_{22}c_{44} - 12c_{22}c_{55} - 12c_{22}c_{66} + 23c_{23}^2 - 16c_{23}c_{33} + 12c_{23}c_{44} + 12c_{23}c_{55} \right. \\ \left. + 12c_{23}c_{66} + 60c_{24}^2 - 60c_{24}c_{34} + 60c_{25}^2 - 60c_{25}c_{35} + 60c_{26}^2 - 60c_{26}c_{36} + 8c_{33}^2 - 12c_{33}c_{44} - 12c_{33}c_{55} - 12c_{33}c_{66} \right. \\ \left. + 60c_{34}^2 + 60c_{35}^2 + 60c_{36}^2 + 72c_{44}^2 - 36c_{44}c_{55} - 36c_{44}c_{66} + 180c_{45}^2 + 180c_{46}^2 + 72c_{55}^2 - 36c_{55}c_{66} + 180c_{56}^2 + 72c_{66}^2 \right)$$

and

$$\beta = \frac{32}{3} \left( c_{11}^2 + c_{11}c_{12} + c_{11}c_{13} - c_{11}c_{22} - 2c_{11}c_{23} - c_{11}c_{33} + c_{12}^2 - c_{12}c_{13} + c_{12}c_{22} - c_{12}c_{23} - 2c_{12}c_{33} + c_{13}^2 - 2c_{13}c_{22} - c_{13}c_{23} + c_{13}c_{33} + 3c_{14}^2 + 6c_{14}c_{24} + 6c_{14}c_{34} + 3c_{15}^2 + 6c_{15}c_{25} + 6c_{15}c_{35} + 3c_{16}^2 + 6c_{16}c_{26} + 6c_{16}c_{36} + c_{22}^2 + c_{22}c_{23} - c_{22}c_{33} + c_{23}^2 + c_{23}c_{33} + 3c_{24}^2 + 6c_{24}c_{34} + 3c_{25}^2 + 6c_{25}c_{35} + 3c_{26}^2 + 6c_{26}c_{36} + c_{33}^2 + 3c_{34}^2 + 3c_{35}^2 + 3c_{36}^2 \right).$$
(7)

Equivalent expressions for the Rayleigh attenuations have been well-known for many years, even for crystal symmetry as low as orthorhombic. However, to the best of the authors' knowledge, the Rayleigh attenuations have not been written explicitly in terms of the bulk and shear moduli anisotropies, which is important for defining the ratio seen in Eq. (1). The Rayleigh attenuation ratio  $\alpha_L^{\rm Rayleigh}/\alpha_S^{\rm Rayleigh}$  can then be written in the form

$$\frac{\alpha_L^{\text{Rayleigh}}}{\alpha_S^{\text{Rayleigh}}} = \frac{4}{3}R^{-3} \left[ 1 + \frac{(2+3R^5)\beta}{2\beta + 2^6 \cdot 3 \cdot 7(2+3R^5)\mu} \right]. \tag{8}$$

Note that Eq. (8) is independent of the correlation length  $\ell$ , a result that was first obtained by Merkulov. Equation (8) enables the primary result of this letter, which is an expression for the bounds on the attenuation ratio.

Next, consider a polycrystal containing crystallites of cubic crystallographic symmetry. The bulk modulus of a single crystallite of cubic symmetry is equal to the bulk modulus of a polycrystal containing the crystallites. Thus, the anisotropy in the bulk modulus vanishes, i.e.,  $\beta = 0$ . The second-order anisotropy in the shear modulus is obtained by applying the symmetry relations for cubic symmetry on Eq. (7), which gives  $\mu = 3(c_{11} - c_{12} - 2c_{44})^2/175$ . Simplifying the resulting Rayleigh attenuations gives

$$\alpha_L^{\text{Rayleigh}} = \frac{4}{375} \frac{\ell^3 \omega^4 (c_{11} - c_{12} - 2c_{44})^2}{\rho^2 c_L^8} (2 + 3R^5)$$
 (9)

and

$$\alpha_S^{\text{Rayleigh}} = \frac{3}{375} \frac{\ell^3 \omega^4 (c_{11} - c_{12} - 2c_{44})^2}{\rho^2 c_S^8} (3 + 2R^{-5}). \quad (10)$$

For this case with  $\beta = 0$ , it is easily seen from Eq. (8) that the ratio of longitudinal to shear wave attenuations simplifies to

$$\frac{\alpha_L^{\text{Rayleigh}}}{\alpha_S^{\text{Rayleigh}}} = \frac{4c_S^3}{3c_L^3},\tag{11}$$

which is exactly the lower-bound derived by Norris. Thus, Eq. (11) is reached when the attenuation results from only the anisotropy in the shear modulus.

Now, consider a polycrystal containing crystallites of symmetry lower than cubic. Elastic stability requires a positive bulk modulus for both the crystallites and the polycrystal. Thus, the second-order anisotropy of the bulk modulus must be positive. Applying  $\beta \ge 0$  and evaluating Eq. (8) gives

$$\frac{\alpha_L^{\text{Rayleigh}}}{\alpha_S^{\text{Rayleigh}}} \ge \frac{4c_S^3}{3c_L^3},\tag{12}$$

which is the sought after inequality given in Eq. (1). Thus, the inequality in Eq. (1) derived for viscoelastic materials by Norris<sup>1</sup> is, in fact, more general. It should be noted that Bhatia<sup>7</sup> was the first to establish the equality in Eq. (11). More recently, Turner<sup>17</sup> arrived at a similar conclusion when considering the diffusion of ultrasound. However, to the best of the authors' knowledge, Eq. (11) has never been designated as a lower bound for the polycrystalline problem until now.

Last, we consider the case when  $\beta > 0$  and  $\mu = 0$ . For this case, it is easily seen that Eq. (8) delivers an upper limit, namely,

$$\frac{\alpha_L^{\text{Rayleigh}}}{\alpha_S^{\text{Rayleigh}}} \le \frac{2c_S^3}{3c_L^3} \left( 4 + 3\frac{c_L^5}{c_S^5} \right). \tag{13}$$

In summary, the results of Eqs. (12) and (13) provides the following bounds on  $\alpha_L^{\rm Rayleigh}/\alpha_S^{\rm Rayleigh}$ ,

$$\frac{4c_S^3}{3c_L^3} \le \frac{\alpha_L^{\text{Rayleigh}}}{\alpha_S^{\text{Rayleigh}}} \le \frac{2c_S^3}{3c_L^3} \left(4 + 3\frac{c_L^5}{c_S^5}\right),\tag{14}$$

which is the primary result of this letter. These bounds apply universally to low frequency attenuation in polycrystals resulting from grain scattering.

### **III. RESULTS AND DISCUSSION**

To illustrate the validity of Eq. (11), the single-crystal elastic constants and densities of 2176 crystalline materials were used to calculate Rayleigh attenuations. The dataset of single-crystal elastic constants were obtained elsewhere 18 using Density Functional Theory. The dataset contains example materials that span all of the seven crystallite symmetry point groups. The two ratios involved in Eq. (11) were calculated for each material and were then aggregated into a scatter plot, which is given in Fig. 1. The marker color indicates the corresponding point symmetry group for that specific material. Additionally, the upper and lower limits are included in Fig. 1. The example materials having cubic symmetry are present along the lower limit  $\alpha_L^{\text{Rayleigh}}/\alpha_S^{\text{Rayleigh}} = 4c_S^3/(3c_L^3)$ . All example materials having symmetry lower than cubic appear above the line  $\alpha_L^{\text{Rayleigh}}/\alpha_S^{\text{Rayleigh}}=4c_S^3/(3c_L^3)$  and fall under the upper limit, which agrees with the primary result of Eq. (14). The range  $0.15 \le \alpha_L^{\text{Rayleigh}}/\alpha_S^{\text{Rayleigh}} \le 0.35$  contains the highest percentage of materials, 68.7%, which is highlighted in the exploded view in Fig. 1. Experimental data accumulated by Papadakis<sup>9</sup> were shown to fall within this range as well.

The Poisson's ratio  $\nu$  for isotropic materials can be written in terms of the longitudinal and shear wave speeds. Here, we note that  $4c_S^3/\left(3c_L^3\right) = \frac{\sqrt{2}}{3}\left[(1-2\nu)/(1-\nu)\right]^{3/2}$ , which further links the Poisson's ratio to the ratio of attenuations. For polycrystals having crystallites of cubic symmetry,  $\alpha_L^{\text{Rayleigh}}/\alpha_S^{\text{Rayleigh}} = (\sqrt{2}/3)\left[(1-2\nu)/(1-\nu)\right]^{3/2}$ , while lower symmetries are restricted by the bounds given in Eq. (14). The possible values of Poisson's ratio span  $0.5 \le \nu \le -1$ . Thus, the attenuation ratio is completely bounded from above and below by Eq. (14) and from the left and the right by  $0 \le 4c_S^3/\left(3c_L^3\right) \le \sqrt{3}/2$ . Values of Poisson's ratio that are deemed relevant are included in Fig. 1. As expected, most materials are observed near  $\nu = 0.25$ .

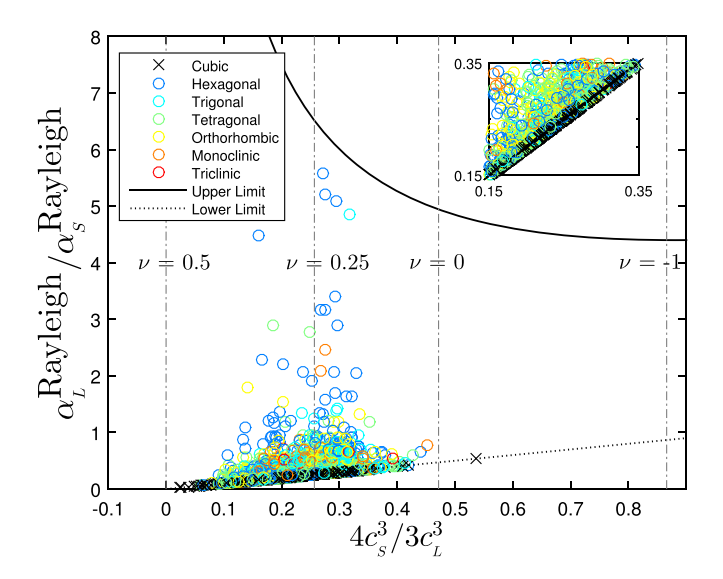


FIG. 1. (Color online) Scatter plot showing the relation between the Rayleigh attenuation ratio and the quantity  $4c_5^3/3c_L^3$ . The lower and upper limits given in Eq. (14) and lines indicating the corresponding Poisson's ratio are included.

The results contained in this letter have considered the low-frequency Rayleigh attenuations. For intermediate frequencies, in the so-called stochastic scattering regime, the integrations involved in Eqs. (2) and (3) are much more complex, which makes it difficult to observe bounds (if any) on  $\alpha_L^{\rm Stochastic}/\alpha_S^{\rm Stochastic}$ . For high frequencies, in the geometrical scattering regime, it is predicted that  $\alpha_L^{\rm Geometric}=\alpha_S^{\rm Geometric}$   $\approx 1/\ell$ , which gives the ratio  $\alpha_L^{\rm Geometric}/\alpha_S^{\rm Geometric}=1$ .

Last, these results are expected to have implications on the multiple scattering and diffusion of ultrasonic waves. Turner<sup>17</sup> showed that, for low-frequencies, the attenuation ratio is proportional to the ratio of the diffusion mean free path  $\alpha_L^{\text{Rayleigh}}/\alpha_S^{\text{Rayleigh}}=\ell_S/\ell_L$  with  $\ell_L$  and  $\ell_P$  being the longitudinal and shear wave mean free paths, respectively. The diffusion mean free path is the average spatial distance between scattering events in the multiple scattering limit. Thus, Eq. (14) additionally bounds the ratio of the mean free paths and places new constraints on the diffusive nature of polycrystals.

## **IV. CONCLUSION**

In this letter, the ratio of low frequency longitudinal and shear wave attenuation constants was proven to be bounded from above and below by certain ratios of the corresponding wave speeds. The lower bound was shown to be equal to the bound derived for viscoelastic materials. In addition, an upper bound to the attenuation ratio was discovered. The upper and lower bounds correspond to the situations when the second-order anisotropy in the shear and bulk modulus goes to zero, i.e., the shear/bulk modulus of a single crystallite in the polycrystal is equal to the shear/bulk modulus of the polycrystal. This feature parallels the finding for viscoelastic materials that the lower bound is met when the absorption of a wave is only caused by the shear modulus. An analysis of the attenuation ratio for 2176 materials, generated using Density Functional Theory, was conducted to test the validity of the bounds. All data points were observed to fall within the bounds. This analysis highlighted the relation of the ratio of attenuations to the Poisson's ratio. The possible values of the Poisson's ratio further bounds the ratio of attenuations from the left and to the right. Further work will be explored that will involve experimental confirmation and extensions to other frequencies and attenuation mechanisms.

## **ACKNOWLEDGMENTS**

The authors would like to gratefully acknowledge Maarten de Jong for sharing the single-crystal elastic constant data generated from his Density Functional Theory calculations. The research reported in this document was performed under contract(s)/instrument(s) W911QX-16-D-0014 and W911QX-13-D-0003 with the U.S. Army Research Laboratory. The views and conclusions contained in this document are those of Bennett Aerospace and the U.S. Army Research Laboratory. The citation of manufacturer's or trade names does not constitute an official endorsement or approval of the use thereof. The U.S. Government is authorized to reproduce and distribute reprints for Government purposes notwithstanding any copyright notation hereon.

- <sup>1</sup>A. N. Norris, "An inequality for longitudinal and transverse wave attenuation," J. Acoust. Soc. Am. **141**, 475–479 (2017).
- <sup>2</sup>R. Truell, C. Elbaum, and B. B. Chick, *Ultrasonic Methods in Solid State Physics* (Academic Press, New York 1969), 464 pp.
- <sup>3</sup>W. P. Mason and H. J. McSkimin, "Attenuation and scattering of high frequency sound waves in metals and glasses," J. Acoust. Soc. Am. **19**, 464–473 (1947)
- <sup>4</sup>W. P. Mason and H. J. McSkimin, "Energy losses of sound waves in metals due to scattering and diffusion," J. Appl. Phys. 19, 940–946 (1948).
- <sup>5</sup>E. M. Lifshits and G. D. Parkhamovski, "Theory of propagation of supersonic waves in polycrystals," Zh. Eksp. Teor. Fiz. 20, 175–182 (1950) (in Russian).
   <sup>6</sup>L. G. Merkulov, "Study of the scattering of ultrasound in metals," Zh. Tekh. Fiz. 26, 64–75 (1956) (English translation).
- <sup>7</sup>A. B. Bhatia, "Scattering of high-frequency sound waves in polycrystal-line materials," J. Acoust. Soc. Am. **31**, 16–23 (1959).
- <sup>8</sup>A. B. Bhatia and R. A. Moore, "Scattering of high-frequency sound waves in polycrystalline materials. II," J. Acoust. Soc. Am. 31, 1140–1142 (1959).
   <sup>9</sup>E. P. Papadakis, "Ultrasonic attenuation caused by scattering in polycrystalline media," in *Physical Acoustics: Principles and Methods*, edited by
- W. P. Mason (Academic Press, New York, 1968), Vol. 4B, pp. 269–328.
  <sup>10</sup>F. E. Stanke and G. S. Kino, "A unified theory for elastic wave propagation in polycrystalline materials," J. Acoust. Soc. Am. 75, 665–681 (1984).
- <sup>11</sup>R. L. Weaver, "Diffusivity of ultrasound in polycrystals," J. Mech. Phys. Solids 38, 55–86 (1990).
- <sup>12</sup>C. M. Kube and J. A. Turner, "Acoustic attenuation coefficients for polycrystalline materials containing crystallites of any symmetry class," J. Acoust. Soc. Am. 137, EL476–EL482 (2015).
- <sup>13</sup>X.-G. Zhang, W. A. Simpson, Jr., J. M. Vitek, D. J. Barnard, L. J. Tweed, and J. Foley, "Ultrasonic attenuation due to grain boundary scattering in copper and copper-aluminum," J. Acoust. Soc. Am. 116, 109–116 (2004).
- <sup>14</sup>A. Van Pamel, C. R. Brett, P. Huthwaite, and M. J. S. Lowe, "Finite element modelling of elastic wave scattering within a polycrystalline material in two and three dimensions," J. Acoust. Soc. Am. 138, 2326–2336 (2015).
- <sup>15</sup>S. I. Rokhlin, J. Li, and G. Sha, "Far-field scattering model for wave propagation in random media," J. Acoust. Soc. Am. 137, 2655–2669 (2015).
- <sup>16</sup>M. Calvet and L. Margerin, "Velocity and attenuation of scalar and elastic waves in random media: A spectral function approach," J. Acoust. Soc. Am. 131, 1843–1862 (2012).
- <sup>17</sup>J. A. Turner, "Scattering and diffusion of seismic waves," Seismol. Soc. Am. Bull. 88, 276–283 (1998).
- <sup>18</sup>M. de Jong, W. Chen, T. Angsten, A. Jain, R. Notestine, A. Gamst, M. Sluiter, C. Krishna Ande, S. van der Zwaag, J. J. Plata, C. Toher, S. Curtarolo, G. Ceder, K. A. Persson, and M. Asta, "Charting the complete elastic properties of inorganic crystalline compounds," Nature Scientific Data 2, 150009 (2015).